International Journal of Thermophysics, Vol. 27, No. 6, November 2006 (© 2006)
DOI: 10.1007/s10765-006-0089-3

Thermal Conductivity Measurements of Liquid Mercury and Gallium by a Transient Hot-Wire Method in a Static Magnetic Field[1]

H. Fukuyama,[2,3] T. Yoshimura,[4] H. Yasuda,[5] and H. Ohta[6]

The transient hot-wire method, incorporating a static magnetic field, has been developed to measure thermal conductivities of liquid mercury and gallium. Prior to the measurements, the effect of an alumina-coated hot wire on the measurements has been evaluated. Natural convection in the liquid metals has been effectively suppressed by the Lorentz force acting on the liquid metals in a static magnetic field. The thermal conductivities of liquid mercury and gallium have been determined to be 7.9 $W \cdot m^{-1} \cdot K^{-1}$ at 291 K and 24 $W \cdot m^{-1} \cdot K^{-1}$ at 302.9 K, respectively.

KEY WORDS: gallium; mercury; static magnetic field; thermal conductivity; transient hot wire method.

1. INTRODUCTION

Thermal conductivities of high-temperature melts are one of the most important thermophysical properties in addition to the heat capacity, density, viscosity, and surface tension for improvement of process control and

[1]Paper presented at the Seventeenth European Conference on Thermophysical Properties, September 5–8, 2005, Bratislava, Slovak Republic.

[2]Institute of Multidisciplinary Research for Advanced Materials (IMRAM), Tohoku University, 2-1-1 Katahira, Aoba, Sendai 980-8577, Japan.
[3]To whom correspondence should be addressed. E-mail: fukuyama@tagen.tohoku.ac.jp
[4]Department of Chemistry and Materials Science, Tokyo Institute of Technology, 2-12-1 Ookayama, Meguro, Tokyo 152-8552, Japan.
[5]Department of Adaptive Machine Systems, Osaka University, 2-1 Yamadaoka, Suita, Osaka 565-0871, Japan.
[6]Department of Materials Science, Ibaraki University, 4-12-1 Hitachi, Ibaraki 316-8511, Japan.

process simulation [1]. However, measurements of the thermal conductivity of a liquid metal involve experimental difficulties caused by natural convection and Marangoni flow. A microgravity condition is an ideal field to suppress the convection caused by a buoyancy force. From this point of view, Hibiya et al. measured the thermal conductivity of molten InSb under microgravity using the TEXUS-24 rocket [2] and the drop shaft facility (microgravity of 10^{-5} g for 10 s), Japan Microgravity Centre (JAMIC) [3, 4]. Nagai et al. [5, 6] measured the thermal conductivity of molten mercury and silicon under microgravity of 10^{-3} g for 1.2 s using the short-duration drop tower facility of the Hokkaido National Industrial Research Institute (HNIRI), Japan. Nagata and Fukuyama [7] measured the thermal conductivity of aluminium, nickel, and silicon melts by means of a transient hot wire method under microgravity of 10^{-5} g using the drop shaft facility, JAMIC. However, their results were much smaller than any other values previously reported. In their experiments, a molybdenum wire was used as a heating wire and coated with alumina by electrophoretic deposition to prevent electric current leakage through the melts. The effect of the insulation coating on the thermal conductivity values should be quantitatively evaluated for further discussion.

On the other hand, Nakamura et al. [8] conducted pioneering work utilizing a static magnetic field. They measured the thermal conductivity of liquid mercury in a static magnetic field and experimentally confirmed the effective suppression of natural convection by the Lorentz force. In their experiments, a transient method was employed using a platinum wire printed on an alumina substrate. The wire was coated with a 60-μm- alumina insulation layer. The convection seems to be successfully suppressed in a static magnetic field. However, an effect of the alumina insulation layer on the measurements might still remain.

In the present study, the transient hot-wire method, incorporating a static magnetic field, has been developed for precise measurements of thermal conductivities of molten metals. The measurements were conducted on liquid mercury and liquid gallium. Prior to the measurements, the effect of an alumina-coated hot wire on the measurements is quantitatively evaluated [9]. Based on the calculated results, suitable experimental conditions are chosen for the thermal conductivity measurements.

2. THEORY

2.1. Principle of Transient Hot-Wire Method

Based on the solution of a continuous line source of heat, the temperature increase in a line source at time t is given for large values of t

by the following equation [10]:

$$\Delta T = \frac{q}{4\pi\lambda}\ln\left(\frac{4at}{r^2}\right) - \frac{\gamma q}{4\pi\lambda}, \tag{1}$$

where ΔT is the increase in the temperature of the hot wire,q is the heat generation rate per unit length of the line source, λ is the thermal conductivity, a is the thermal diffusivity, r is the radius, and γ is the Euler's constant. The symbols are summarized in the Nomenclature. Differentiating Eq. (1) with respect to the natural logarithm of time, ln t, gives the following equation,

$$\frac{\partial \Delta T}{\partial \ln t} = \frac{q}{4\pi\lambda}. \tag{2}$$

The thermal conductivity of a liquid, in which the line source is placed, is, therefore, determined by the following equation:

$$\lambda = \frac{q}{4\pi\left(\frac{\partial \Delta T}{\partial \ln t}\right)} \tag{3}$$

The above equation is valid only for an ideally thin line source (hot wire) carrying an electric current and heating an infinite substance. In the present study, an alumina-coated hot wire is used to prevent electric current leakage through metallic melts as shown in Fig. 1. Figure 2 presents a cross-sectional view of the alumina-coated hot wire. The effect of the alumina insulation layer on the thermal conductivity measurements is explained in the next section.

2.2. Effect of Alumina Insulation Layer on Thermal Conductivity Measurements

To evaluate the effect of the alumina-coated hot wire on the thermal-conductivity measurements, the following equations of conduction of heat through a hot wire to a liquid metal should be considered. The equations are expressed in cylindrical coordinates as shown in Fig. 2 where the temperature is a function of radius, r, and t as in Ref. [11];

(1) Hot wire

$$\frac{\partial^2 \Delta T_1}{\partial r^2} + \frac{1}{r}\frac{\partial \Delta T_1}{\partial r} - \frac{1}{a_1}\frac{\partial \Delta T_1}{\partial t} = -\frac{q}{\pi r_i^2 \lambda_1} \quad (0 \le r \le r_i) \tag{4}$$

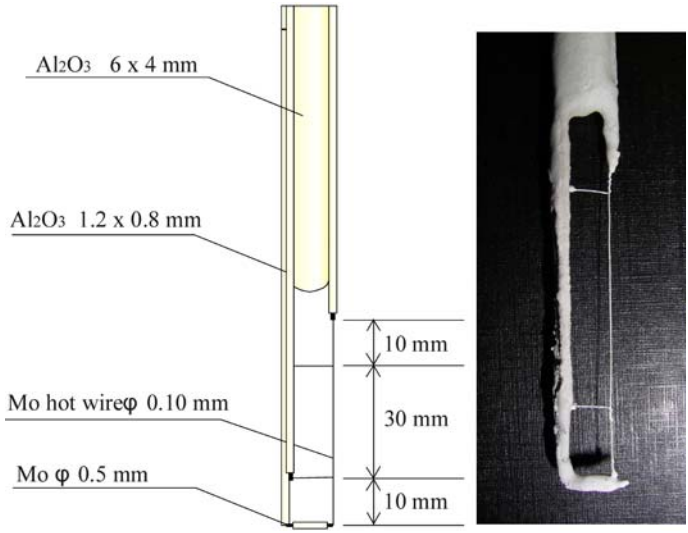

Fig. 1. Left: Schematic diagram of the probe for the thermal conductivity measurement. Right: Photograph of the alumina-coated Mo hot wire.

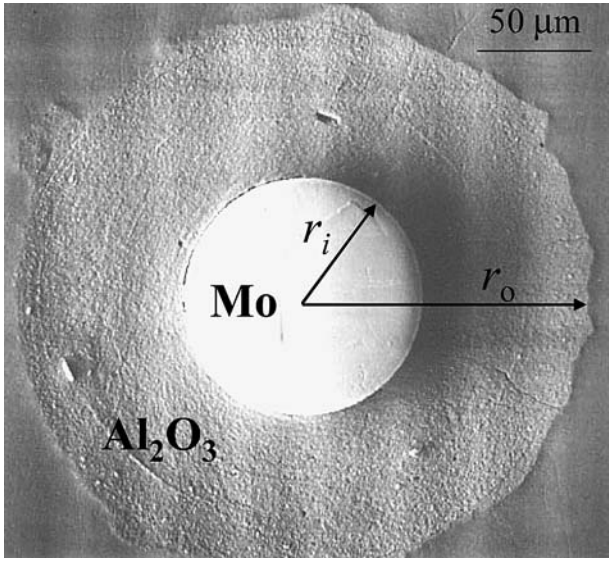

Fig. 2. Cross-sectional view of the hot wire coated with the alumina insulator.

(2) Alumina insulation layer

$$\frac{\partial^2 \Delta T_2}{\partial r^2} + \frac{1}{r}\frac{\partial \Delta T_2}{\partial r} - \frac{1}{a_2}\frac{\partial \Delta T_2}{\partial t} = 0 \quad (r_i \le r \le r_o) \tag{5}$$

(3) Liquid metal

$$\frac{\partial^2 \Delta T_3}{\partial r^2} + \frac{1}{r}\frac{\partial \Delta T_3}{\partial r} - \frac{1}{a_3}\frac{\partial \Delta T_3}{\partial t} = 0 \quad (r_o \le r) \tag{6}$$

Initial condition

$$\Delta T_1 = \Delta T_2 = \Delta T_3 = 0 \quad (t \le 0) \tag{7}$$

Boundary conditions

$$\lambda_1 \frac{\partial \Delta T_1}{\partial r} = \lambda_2 \frac{\Delta T_2}{\partial r} \quad (r = r_i) \tag{8}$$

$$\Delta T_1 = \Delta T_2 \quad (r = r_i) \tag{9}$$

$$\lambda_2 \frac{\partial \Delta T_2}{\partial r} = \lambda_3 \frac{\Delta T_3}{\partial r} \quad (r = r_o) \tag{10}$$

$$\Delta T_2 = \Delta T_3 \quad (r = r_o) \tag{11}$$

$$\Delta T_3 = 0 \quad (r \to \infty). \tag{12}$$

Solving Eqs. (4–6) using initial and boundary conditions, Eqs. (7–12), gives the temperature change of the hot wire, ΔT_1. The average temperature of the hot wire, $\Delta \overline{T_1}$, is obtained by integrating ΔT_1 with respect to the radius as

$$\Delta \overline{T_1} = \int_0^{r_i} \Delta T_1 \frac{2r}{r_i^2}\, \mathrm{d}r = \frac{q}{4\pi\lambda_3}\left\{\ln t + D + \frac{1}{t}(E \ln t + F)\right\}, \tag{13}$$

where functions D, E, and F are expressed by

$$D = \ln\frac{4a_3}{r_o^2 c} + \frac{2\lambda_3}{\lambda_2}\ln\frac{r_o}{r_i} + \frac{\lambda_3}{2\lambda_1}, \quad E = \frac{1}{2\lambda_3}\left\{r_i^2\left(\frac{\lambda_2}{a_2} - \frac{\lambda_1}{a_1}\right) + r_o^2\left(\frac{\lambda_3}{a_3} - \frac{\lambda_2}{a_2}\right)\right\}$$

$$F = \frac{r_i^2}{8}\left\{\left(\frac{\lambda_3-\lambda_2}{\lambda_1}\right)\left(\frac{1}{a_1}-\frac{1}{a_2}\right)+\frac{4}{a_2}-\frac{2}{a_1}\right\}+\frac{r_o^2}{2}\left(\frac{1}{a_3}-\frac{1}{a_2}\right)$$
$$+\frac{r_i^2}{\lambda_2}\left(\frac{\lambda_2}{a_2}-\frac{\lambda_1}{a_1}\right)\ln\frac{r_o}{r_i}+\frac{1}{2\lambda_3}\left\{r_i^2\left(\frac{\lambda_2}{a_2}-\frac{\lambda_1}{a_1}\right)+r_o^2\left(\frac{\lambda_3}{a_3}-\frac{\lambda_2}{a_2}\right)\right\}\ln\frac{4a_3}{r_o^2 c}. \tag{14}$$

Differentiating Eq. (13) with respect to $\ln t$ gives the following equation:

$$\frac{\partial \Delta\overline{T_1}}{\partial \ln t} = \frac{q}{4\pi\lambda_3}\left\{1+\frac{E}{t}-\frac{1}{t}(E\ln t+F)\right\}. \tag{15}$$

Therefore, the thermal conductivity of a liquid determined by using an alumina-coated hot wire is expressed by

$$\lambda_3 = \frac{q}{4\pi\left(\frac{\partial\Delta\overline{T_1}}{\partial\ln t}\right)}\left\{1+\frac{E}{t}-\frac{1}{t}(E\ln t+F)\right\}. \tag{16}$$

Equation (16) contains functions E and F, which are functions of the thermophysical properties of the alumina insulation layer and properties of the hot wire and liquid. Therefore, the thermophysical properties of the insulation layer are necessary to evaluate the effect of the alumina layer on the thermal conductivity measurement. The characteristics of the insulation layer as experimentally determined are described in the next section.

3. EXPERIMENTAL

3.1. Electrophoretic Deposition for Alumina Insulation Layer

Figure 1 shows the probe used for thermal conductivity measurements using the transient hot wire method. A molybdenum wire (diameter of 100 μm) was used as the hot wire. The hot wire was coated with an alumina layer by electrophoretic deposition to prevent electrical current leakage through the liquid metal. The specific details of the electrophoretic deposition are described below [12].

A 99.9% pure alumina powder (size of 0.50μm) was suspended in an ethanol–water solution containing $Al(NO_3)_3$, $(CH_3)_2CHOH$, and $CH_3COC_2H_5$. The hot wire and an aluminium plate were immersed in the alumina suspension as cathode and anode electrodes, respectively. A dc electric voltage of 100 V was applied for a period from 10 to 30 s between both electrodes. The suspension was stirred with a magnetic stirrer during the deposition. The alumina particles were deposited on the wire, and the thickness of the alumina layer varied from 40 to 70 μm. A typical cross-sectional view of the alumina layer on the molybdenum wire is presented in Fig. 2.

3.2. Density and Thermal Effusivity of Alumina Insulation Layer

In order to evaluate the effect of the alumina layer on the thermal conductivity measurements, the density and thermal effusivity of the layer should be determined. For this purpose, an alumina layer was prepared on a molybdenum plate (thickness of 0.15 mm) by electrophoretic deposition. After that, the alumina layer was dried for 86.4 ks (24 h) at room temperature in air. The density of the layer was determined using the mass increase during the deposition and its volume estimated from a cross-sectional photograph of the layer.

The thermal effusivity of the alumina layer was determined by a thermoreflectance method. Since the experimental details of the thermoreflectance method were explained elsewhere [13], only a brief outline is explained below. A molybdenum thin film (thickness of 100 nm) sputtered on the surface of the alumina layer was periodically heated by a laser diode with a wavelength of 830 nm, and the temperature response was measured using a He–Ne laser as a thermoreflectance signal. The surface temperature was estimated from the reflectance of the molybdenum thin film. The thermal effusivity of the sample was derived from the phase lag of the temperature response from modulation heating. The thermal effusivity, b, is defined as

$$b = \sqrt{\rho c_p \lambda}, \tag{17}$$

where ρ is the density and c_p is the heat capacity per unit mass. Single crystalline α-Al_2O_3, silicon, and Pyrex glass were used as standard samples for the measurement.

3.3. Transient Hot-Wire Method in Static Magnetic Field

Figure 3 shows a schematic of the experimental setup. Mercury (purity of 99.5 mass%) or gallium (purity of 99.99 mass%) was held in a glass container (inner diameter of 70 mm) and the container was placed in the bore of a helium-free superconducting magnet (bore radius of 100 mm). The probe for the thermal conductivity measurements was set vertically in the melt. A Teflon disc was placed on the top of the melt to suppress Marangoni flow. A static magnetic field up to 5 T was applied. A constant electric current is supplied to the hot wire placed in the liquid metal. The appropriate currents were pre-experimentally determined to be 2.5 A for mercury and 3.5 A for gallium. The variation of temperature of the hot wire was determined as the variation of the electric voltage due to its electric resistance change by means of a four-terminal method. The data were recorded by using a data logger with a

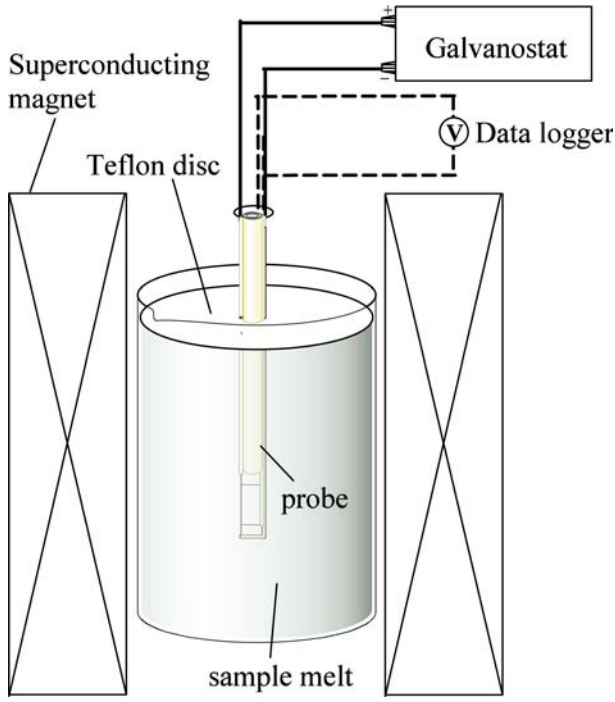

Fig. 3. Experimental setup for the thermal conductivity measurement of liquid metals in a static magnetic field.

resolution of 14 bit and a sampling interval of 1 ms. The thermal conductivity of mercury was measured at 291 K. For liquid gallium, thermal conductivities were measured at temperatures ranging from 302.9 to 331 K by heating the melt with a ribbon heater.

4. RESULTS

4.1. Effect of Alumina Insulation Layer on Thermal Conductivity

The density of the alumina layer has been determined to be $(2.2 \pm 0.2) \times 10^3\,\mathrm{kg \cdot m^{-3}}$. This value is almost half of the value for sintered alumina [14]. This is because the alumina layer was only dried at room temperature in air for 86.4 ks (24 h), and, therefore, densification was not fully attained. The thermal effusivities of the alumina layer were widely scattered due to surface roughness, and varied from 130 to $860\,\mathrm{J \cdot s^{-1/2} \cdot m^{-2} \cdot K^{-1}}$. These values correspond to variations of 0.01–0.43 $\mathrm{W \cdot m^{-1} \cdot K^{-1}}$ in the thermal conductivity, which were determined using Eq. (17). These values are much

lower than the value for sintered alumina [14]. Thus, the large variation in thermal effusivity is caused by surface roughness, and the difference in thermal conductivity between the alumina layer and sintered alumina is caused by the difference in density. The average thermal conductivity of $0.16\,W{\cdot}m^{-1}{\cdot}K^{-1}$ is used for studying the effect of the alumina layer. The maximum effects on the thermal conductivities of both mercury and gallium when using the value of $0.01\,W{\cdot}m^{-1}{\cdot}K^{-1}$ as the thermal conductivity of the alumina layer are also evaluated in Section 4.2. The thermophysical properties of the alumina layer together with those for molybdenum, mercury, and gallium are reported in Table I.

Figure 4 shows the effect of the alumina insulation layer on the thermal conductivities of (a) liquid mercury and (b) liquid gallium estimated using Eqs. (3) and (15). All input data used for the calculation are presented in Table I [15–17]. The calculations were conducted under the conditions of heating currents of 2.5 A at 300 K for liquid mercury and 3.5 A at 302.9 K for liquid gallium. The ordinate in Fig. 4 is the relative thermal conductivity, which is normalized by the recommended value for each melt [15]. The thicker alumina insulation layer yields smaller values of thermal conductivity, and the effect of the insulation layer is especially significant at the initial time periods for both mercury and gallium. The effect reduces with time, and the value of thermal conductivity approaches a true value.

Figure 5 shows the experimentally obtained effects of the alumina insulation on the thermal conductivity of mercury. The experimental results exhibit similar behavior to the predicted results. However, natural convection occurred during the course of the thermal conductivity measurements due to the non-steady heat generated by the hot wire before the thermal conductivity reaches the true value. Once natural convection occurs, the apparent thermal conductivity will increase rapidly as shown in Fig. 5. Therefore, suppression of natural convection is essentially required.

4.2. Thermal Conductivities under Various Magnetic Fields

Figure 6 shows the temperature increase in the hot wire, ΔT with logarithm of t for (a) liquid mercury and (b) liquid gallium under various magnetic fields. The linear relationship deteriorates in the longer time region under a static magnetic field of 0 T due to natural convection. However, with an increasing static magnetic field, the linearity becomes better, because the natural convection is effectively suppressed by the Lorentz force caused by the static magnetic field.

Table I. Thermophysical Properties of Molybdenum Hot Wire, Alumina Insulator, and Sample Melts (Hg and Ga)

	Mo (300 K)	Ref.	Hg (300 K)	Ref.	Ga (302.9 K)	Ref.	alumina insulator	Ref.
Thermal conductivity ($W \cdot m^{-1} \cdot K^{-1}$)	138	[15]	8.3	[15]	28.1	[15]	0.16 (0.01-0.43)	Present work
Heat capacity per unit mass ($J \cdot kg^{-1} \cdot K^{-1}$)	2.50×10^2	[16]	1.39×10^2	[16]	4.09×10^2	[16]	7.80×10^2	[16]
Density ($kg \cdot m^{-3}$)	1.02×10^4	[17]	1.35×10^4	[17]	6.09×10^3	[17]	2.20×10^3	Present work
Viscosity (Pa·s)			1.52×10^{-3}	[17]	2.04×10^{-3}	[17]		
Resistivity (Ω·m)			9.64×10^{-7}	[17]	2.60×10^{-7}	[17]		
Volumetric coefficient of expansion (K^{-1})			1.80×10^{-4}	[17]	9.85×10^{-5}	[17]		

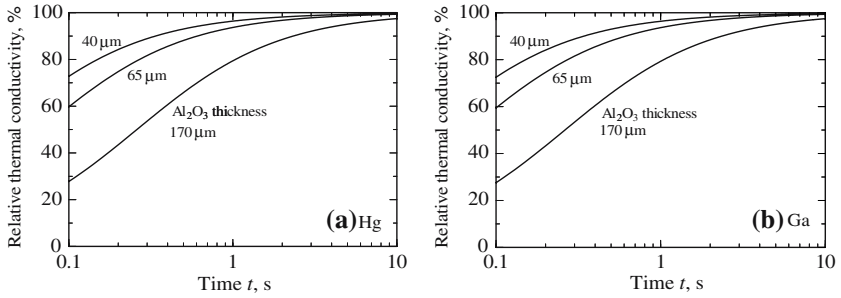

Fig. 4. Evaluation of effects of the alumina insulator on the thermal conductivity measurements of (a) liquid Hg at 300 K and (b) liquid Ga at 302.9 K. The calculation was conducted under the condition of an electric current of 2.5 A for liquid Hg and 3.5 A for liquid Ga.

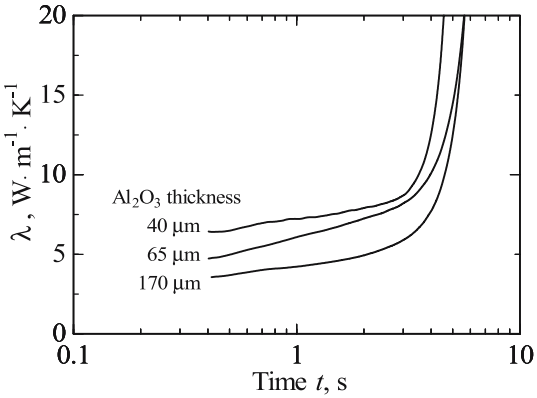

Fig. 5. Experimental results for investigating the effect of an alumina insulator on the thermal conductivity measurement of liquid Hg at a current of 2.5 A at room temperature without magnetic field.

Figure 7 shows the thermal conductivities of (a) liquid mercury and (b) liquid gallium obtained from the slope presented in Fig. 6 using Eq. (3). At the beginning of the measurements, the thermal conductivities gradually increased due to the effect of the alumina insulation layer. After that, natural convection took place and the thermal conductivity rapidly increased under a magnetic field of 0 T. The threshold time for natural convection occurrence was delayed as the static magnetic field was applied.

A constant value for the thermal conductivity of mercury was attained at 4 s under a magnetic field of 5.0 T. Comparing Fig. 4a with Fig. 7a, the thermal conductivity of mercury attains over 99% of its true value at 4 s. Therefore, the thermal conductivity of mercury has been determined to be

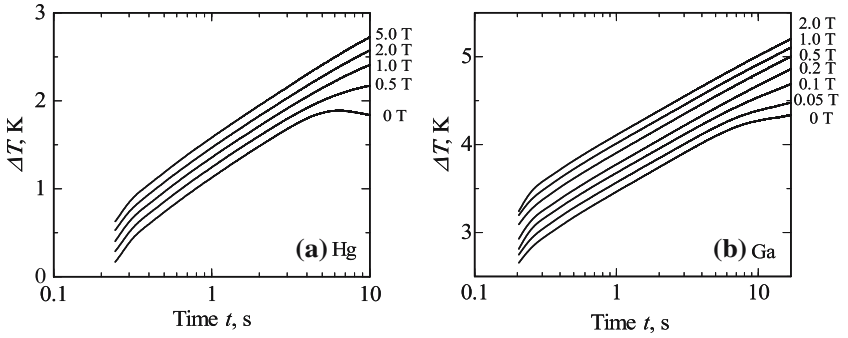

Fig. 6. Temperature increase in hot wire with logarithm of time for various magnetic fields for (a) liquid Hg at 291 K and (b) liquid Ga at 302.9 K. Alumina coating thickness: 40μm; electric current: 2.5 A for liquid Hg. Alumina coating thickness: 70μm; electric current: 3.5 A for liquid Ga.

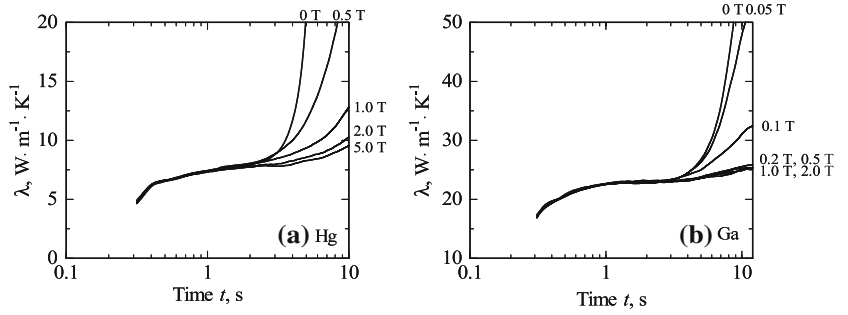

Fig. 7. Variation of thermal conductivity with logarithm of time for various magnetic fields for (a) liquid Hg at 291 K and (b) liquid Ga at 302.9 K. Alumina coating thickness: 40μm; electric current: 2.5 A for liquid Hg. Alumina coating thickness: 70μm; electric current: 3.5 A for liquid Ga.

7.9 $W \cdot m^{-1} \cdot K^{-1}$ at 291 K with the negligible effects of natural convection. However, the maximum experimental uncertainty would be evaluated to be 13% when taking into account the variation in the thermal conductivity of the alumina insulation layer presented in the preceding section.

The behavior of the thermal conductivity of liquid gallium is similar to that of mercury. The thermal conductivity gradually increased during the initial stage due to the effect of the alumina insulation layer. Then, natural convection commenced at 3 s under a static magnetic field of 0 T. When a static magnetic field (1.0–2.0 T) was imposed to gallium, the natural convection was suppressed. A constant value of the thermal conductivity of gallium remains until the time reaches 5 s. Thus, the thermal

conductivity of gallium was determined to be $24\,W \cdot m^{-1} \cdot K^{-1}$ at 302.9 K under a magnetic field of 2.0 T at 5 s, which is close to 99% of its true value from Fig. 4b. However, the maximum experimental uncertainty would be evaluated to be 18% when taking into account the variation in the thermal conductivity of the alumina insulation layer. A relatively smaller magnetic field was required for suppression of convection for the case of gallium compared with mercury. This is amplified in Section 5.

4.3. Comparisons with Previous Data

Figure 8 shows comparisons of the present result for liquid mercury with previous data reported by several authors [8, 18–25]. The present result agrees reasonably with previous results including those obtained under microgravity conditions [18, 19]. Nakamura et al. [8] conducted pioneering work using a static magnetic field up to 4 T at 269 K. All results are distributed along the curve calculated from the Wiedemann–Franz law except for the results obtained by Peralta et al. [20].

Figure 9 shows the temperature dependence of the thermal conductivity of liquid gallium compared with previous results obtained by several investigators [26–30]. All results exhibit positive temperature dependenc-

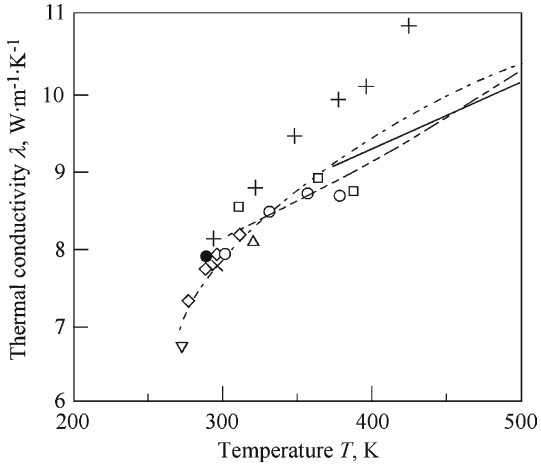

Fig. 8. Thermal conductivity of liquid Hg as a function of temperature along with results reported by other investigators. *Transient hot-wire method:*●, Present study; ▽, Nakamura et al. (Magnetic field) [8]; ◯, Nakamura et al. (μg) [18]; □, Nakamura et al. (μg) [19]; +, Peralta et al. [20]; ◇ Yamasue et al. [21]; ×, Brooks et al. [22]. Laser-Pulse method: – - –, Schriempf [23]; Axial heat flow method: ——, Duggin [24]; △, Sundquist [25]; - – - –, Calculated from W-F law.

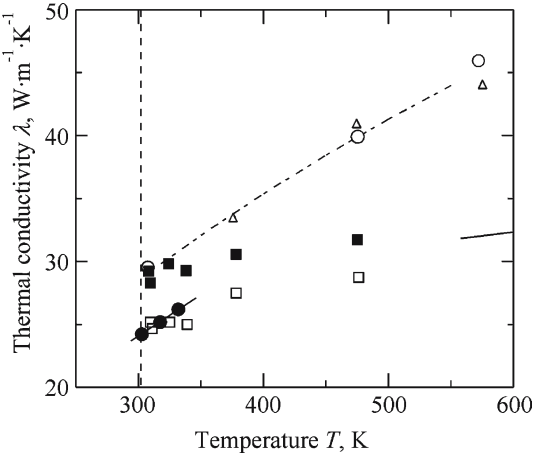

Fig. 9. Thermal conductivity of liquid Ga as a function of temperature along with results reported by other investigators. Transient hot-wire method. •, Present study; ■, relative technique Miyamura and Susa [26]; □, absolute technique Miyamura and Susa [26]; - - - -, Recommended value [27]; - – - – -, Calculated form w-F law; —— Gamazov [30]. Laser-pulse mehod; △, Schriempf [28]; Axial heat flow method: ◯, Magmedov [29].

es. Miyamura and Susa [26] obtained the thermal conductivities of liquid gallium by means of the transient hot-wire method using an alumina-coated hot wire. They corrected their results to avoid the effects of the insulation layer using the value recommended by the National Physical Laboratory (NPL) [27], which was $28\,\mathrm{W\cdot m^{-1}\cdot K^{-1}}$ at the melting point of Ga. This technique was referred to as a "relative technique." The present study agrees with their original values rather than the corrected ones. The values of the present results are somewhat smaller than the results obtained by Schriempf [28] and Magmedov [29]. This difference may be caused by complete suppression of both natural and Marangoni convections during the course of measurements in the present study.

5. DISCUSSION

The expression of the Rayleigh number, Ra, for line source heating was derived by van der Held and van Drunen [31] as follows:

$$\mathrm{Ra} = \frac{g\beta\rho^2 c_p \Delta T}{\lambda\mu} r_i^3 \left\{ \exp\frac{1}{2}\left(\ln\frac{4\lambda t}{\rho c_p r_i^2} - 0.5772 \right) - 1 \right\}^3 . \tag{18}$$

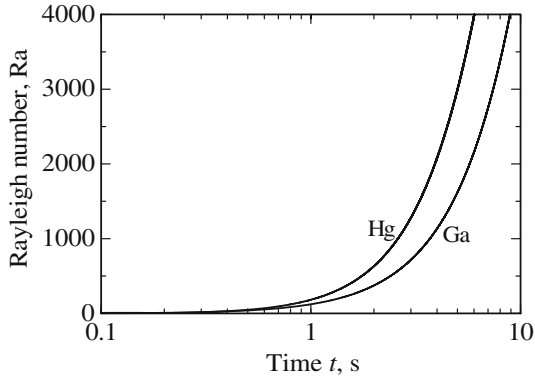

Fig. 10. Variation of Rayleigh number with logarithm of time for liquid Hg and liquid Ga based on the temperature increase in the hot wire without a magnetic field. Alumina coating thickness: 40μm; electric current: 2.5 A for liquid Hg. Alumina coating thickness: 70μm; electric current: 3.5 A for liquid Ga.

The above equation was applied for the present measurements without imposing a magnetic field. Figure 10 shows the variation of the Rayleigh number with the logarithm of time using the thermophysical properties presented in Table I. Van der Held and van Drunen pointed out that the critical point of the convection is $\mathrm{Ra} = 1070$, which corresponds to 2.7 s after passing an electric current of 2.5 A for liquid mercury. For the case of liquid gallium, the critical Ra corresponds to 3.9 s after passing a current of 3.5 A. These critical points agree with the times at which natural convection occurs as shown in Fig. 7.

The extent of suppression of natural convection by a static magnetic field is evaluated using the Hartman number, Ha. An index of suppression of natural convection, Z, is defined by

$$\text{for mercury, } Z = \frac{\lambda(\mathrm{Hg},\ B = x,\ \text{at } 4\,\mathrm{s}) - 7.9}{\lambda(\mathrm{Hg},\ B = 0,\ \text{at } 4\mathrm{s}) - 7.9}, \tag{19}$$

$$\text{for gallium, } Z = \frac{\lambda(\mathrm{Ga}, B = x,\ \text{at } 5\,\mathrm{s}) - 24}{\lambda(\mathrm{Ga}, B = 0,\ \text{at } 5\,\mathrm{s}) - 24}, \tag{20}$$

where $\lambda(i, B = x,\ \text{at } y\ \mathrm{s})$ denotes the thermal conductivity of i under a magnetic field of x T at y s from the beginning of the measurement. The values of 7.9 and 24 in Eqs. (19) and (20) are the thermal conductivities of Hg at 291 K and Ga at 302.9 K, respectively. The value of Z varies from 0 to 1, and $Z = 0$ corresponds to no convection. The Hartman number is

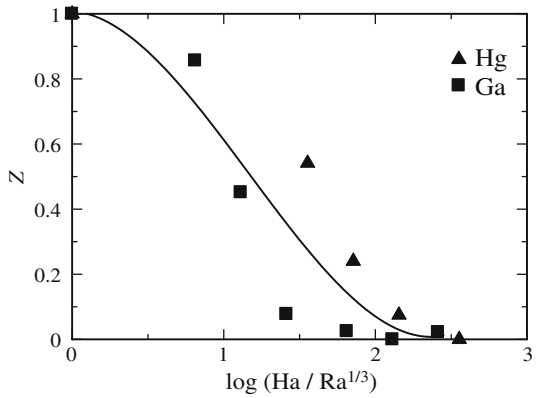

Fig. 11. Variation of Z with dimensionless parameter $Ha/Ra^{1/3}$ for liquid Hg and liquid Ga based on the present results obtained experimentally in various magnetic fields. Alumina coating thickness: 40μm; electric current: 2.5 A for liquid Hg. Alumina coating thickness: 70μm; electric current: 3.5 A for liquid Ga.

defined by

$$\mathrm{Ha} = Bl\left(\frac{\sigma}{\mu}\right)^{1/2}, \tag{21}$$

where l is the radius of the container. The values of Z were plotted against the dimensionless group log ($Ha/Ra^{1/3}$) for both mercury and gallium to evaluate the effectiveness of the Lorentz force as Ozoe and Maruo [32] suggested, which is shown in Fig. 11. An almost smooth correlation curve was obtained, although the difference between mercury and gallium still remains. This means that the Lorentz force acting against natural convection predominantly determines the apparent thermal conductivity, i.e., the rate of heat transfer.

6. CONCLUSIONS

The transient hot-wire method, incorporating a static magnetic field, has been successfully developed to measure the thermal conductivities of liquid mercury and liquid gallium using an alumina-coated hot wire. The natural convection in the liquid metals was effectively suppressed by the Lorentz force in a static magnetic field. The thermal conductivities of liquid mercury and liquid gallium have been determined to be 7.9 $W \cdot m^{-1} \cdot K^{-1}$ at 291 K and 24 $W \cdot m^{-1} \cdot K^{-1}$ at 302.9 K, respectively. However, the thermophysical properties of the insulation layer on the hot wire

should be more precisely determined for the accurate evaluation of the effect on the hot-wire measurements.

7. ACKNOWLEDGMENTS

The authors thank Messrs. H. Nakayama, S. Fujita and H. Ninomiya for their experimental assistance. We wish to thank Prof. I. Ohnaka for the provision of laboratory facilities.

NOMENCLATURE

a:	thermal diffusivity, $m^2 \cdot s^{-1}$
λ:	thermal conductivity, $W \cdot m^{-1} \cdot K^{-1}$
ρ:	density, $kg \cdot m^{-3}$
c_p:	isobaric heat capacity per unit mass, $J \cdot kg^{-1} \cdot K^{-1}$
γ:	Euler's constant, $\gamma = 0.5772 \cdots$
c:	exp $\gamma = 1.781 \cdots$
q:	heat generation rate per unit length of hot wire per unit time, $W \cdot m^{-1}$
t:	time, s
T:	absolute temperature, K
ΔT:	increase in temperature of hot wire, K
g:	acceleration due to gravity, $m \cdot s^{-2}$
B:	magnetic field, T
β:	volumetric coefficient of expansion of liquid metal, K^{-1}
μ:	viscosity of liquid metal, Pa·s
θ:	electric conductivity of liquid metal, $\Omega^{-1} \cdot m^{-1}$
Subscripts	
1:	hot wire
2:	insulator
3:	liquid metal

REFERENCES

1. H. Fukuyama, T. Tsukada, M. Watanabe, T. Tanaka, T. Baba, and T. Hibiya, *J. Japanese Assoc. Crystal Growth* **30**:10 (2003).
2. S. Nakamura, T. Hibiya, F. Yamamoto, and T. Yokota, *Int. J. Thermophys.* **12**:783 (1991).
3. T. Hibiya and S. Nakamura, *Int. J. Thermophys.* **17**:1191 (1996).
4. S. Nakamura and T. Hibiya, *Microgravity Sci. Tech.* **VI/2**:119 (1993).
5. H. Nagai, F. Rossignol, Y. Nakata, T. Tsurue, M. Suzuki, and T. Okutani, *Mater. Sci. Eng. A* **A276**:117 (2000).
6. H. Nagai, Y. Nakata, T. Tsurue, H. Minagawa, K. Kamada, S. Gustafsson, and T. Okutani: *Jpn. J. Appl. Phys*. **39**:1405 (2000).

7. K. Nagata and H. Fukuyama, *Proc. Mills Symp., Metals, Slags, Glasses: High Temp. Props. Phenomena* (The Institute of Materials, London, 2002), pp. 83–91.
8. S. Nakamura, T. Hibiya, T. Yokota, and F. Yamamoto, *Int. J. Heat Mass Transfer* **33**:2609 (1990).
9. H. Fukuyama, T. Yoshimura, H. Yasuda, I. Ohnaka, H. Ohta, H. Nakayama, and N. Taketoshi, *J. Jpn. Soc. Microgravity Appl.* **20**:168 (2003).
10. H. S. Carslaw and J. C. Jaeger, *Conduction of Heat in Solids*, 2nd Ed. (Clarendon Press, Oxford, 1959), pp. 261–263.
11. Y. Nagasaka and A. Nagashima, *Trans. Jpn. Soc. Mech. Eng. B* **47**:1323 (1981).
12. T. Arato, T. Narisawa, N. Koganezawa, and Y. Nonaka, *J. Ceram. Soc. Japan* **100**:75 (1992).
13. N. Taketoshi, M. Ozawa, H. Ohta, and T. Baba, *Proc. 10th Int. Conf. Photoacoustic and Photothermal Phenomena,* F. Scudieri and M. Bertolotti, eds. (The American Institute of Physics, New York, 1999), pp. 315–317.
14. The Japan Institute of Metals *Kinzoku Data Book*, 3rd Ed., (eds) (Maruzen Co., Ltd., Tokyo, 1993), p. 80; referred to W. D. Kingery, *Property Measurements at High Temperatures* (John Wiley, New York, 1959).
15. Y. S. Tououkian, R. W. Powell, C. Y. Ho, and P. G. Klemens, *Thermophysical Properties of Matter*, Vol. 1, *Thermal Conductivity of Metallic Elements and Alloys* (IFI/Plenum Press, New York, 1970).
16. M. W. Chase, Jr., ed., *NIST-JANAF Thermochemical Tables*, 4th Ed. (The American Chemical Society, Washington, DC and the American Institute of Physics, New York, 1998).
17. The Japan Institute of Metals *Kinzoku Data Book*, 3rd Ed., (eds) (Maruzen Co., Ltd., Tokyo, 1993), pp. 15–16; referred to *Metals Reference Book*, 5th Ed. (Butterworths, New York, 1976).
18. S. Nakamura, T. Hibiya, and F. Yamamoto, *J. Appl. Phys.* **68**:5125 (1990).
19. S. Nakamura and T. Hibiya,*Rev. Sci. Instrum.* **59**:2600 (1988).
20. M. V. Peralta, M. Dix, M. Lesemann, and W. A. Wakeham, *High Temp. High Press.* **34**:35 (2002).
21. E. Yamasue, M. Susa, H. Fukuyama, and K. Nagata, *Metall. Mater. Trans. A* **30A**:1971 (1999).
22. R. F. Brooks, B. J. Monaghan, A. J. Barnicoat, A. McCabe, K. C. Mills, and P. N. Quested, *Int. J. Thermophys.* **19**:1151 (1996).
23. J. T. Schriempf, *High Temp. High Press.* **4**:411 (1972).
24. M. J. Duggin, *Proc. 8th Thermal Conductivity Conf.* (Plenum Press, New York, 1969), p. 727.
25. B. Sundqvist, *High Temp. High Press.* **18**:655 (1986).
26. A. Miyamura and M. Susa, *High Temp. High Press.* **34**:607 (2002).
27. K. C. Mills, B. J. Monaghan, and B. J. Keene, *Inter. Mater. Rev.* **41**:209 (1996).
28. J. T. Schriempf, *Solid State Commun.* **13**:651 (1973).
29. A. M. Magmedov, *Tezisy Nauchn. Soobn. Vses Konf. Str. Suoistvan Met Shlak Rasp. 3rd* **2**:21 (1978).
30. A. A. Gamazov, *Sov. Phys. J.* **22**:113 (1979).
31. E. F. M. van der Held and F. G. van Drunen, *Physica* **XV**:865 (1949).
32. H. Ozoe and E. Maruo, *JSME Int. J.* **30**:774 (1987).